Electronic Structure of Polyfluoranthene Ladder Polymers

M. Kertesz* and A. Ashertehrani

Department of Chemistry, Georgetown University, Washington, D.C. 20057-1227

Received August 22, 1995; Revised Manuscript Received October 30, 1995[⊗]

ABSTRACT: Fully unsaturated fluoranthene-type ladder polymers (PFA: polyfluoranthene) recently synthesized by Schlüter et al. show a high degree of π-electron localization. Variation of the size of the two oligoacenic components separated by the characteristic five-membered ring, however, can lead to more delocalized structures with small (few tenths of an electronvolt) band gaps and can be used for engineering the electronic properties. Charge transfer produces bipolaronic defect states in these polymers; sp^3 defects produce polaronic defects. Interpretation of the differences between the published absorption spectra for two members of the PFA family is also given.

1. π-Conjugation in Ladder Polymers

Fully unsaturated ladder fluoranthene-type polymers, which have been recently synthesized by Schlüter et al.,[1,2] consist of cumulated oligoacenic fragments connected by five-membered rings, resembling two-dimensional, flattened, and polymerized buckyballs, or "molecular boards", that contain the characteristic fluoranthene unit and are illustrated in Figure 1. Each polymer is characterized by a p value (number of benzene rings in the perpendicular oligoacenic fragments) and an m value ($m + 1$ is the number of benzene rings in the parallel oligoacenic fragments.) These polyfluoranthene, PFA, polymers are of potential interest for electroluminescence and photovoltaics and join an increasing, albeit still small, group of conjugated polymers with unique ladder topology.[1−6] The most basic electronic and optical parameter of these systems, the band gap, E_g, varies strongly with their topology and structure. In this work we report results concerning the dependence of the structure and the electronic structure, including the band gap, on the makeup of the repeat unit of the polymer. By decomposing[7] E_g into a "topological" and a "relaxation" component, we provide tools for gaining better control over the design of new members of the series.

We also explore related issues:

(1) How does the ladder topology help in maintaining delocalization under the influence of breakages in one "leg" of the ladder structure? This question arises because polymeric ladders are expected to be more sturdy electronically toward interruptions of conjugation, such as those created by the presence of sp^3 carbon defects arising during synthesis.

(2) What type of localized defect structures are generated if additional charges are transferred to the ladder polymer? It has been well established that on single chain conjugated polymers charges tend to localize and generate a deformation of the geometry, producing charged solitons, polarons, and bipolarons.[8] We will attempt to answer the following question: which types of localized charged defects does the ladder topology harbor?

2. Techniques of Calculation

In previous calculations on the electronic structure of conjugated polymers, a good correlation between the calculated and experimental band gap has been achieved only if bond length relaxation has been taken into account.[7,9−12] One of the techniques that has consistently provided good results[11] in terms of agreement with both experiment and other calculations has been the Longuet-Higgins−Salem (LHS) method,[12] which we will employ here.

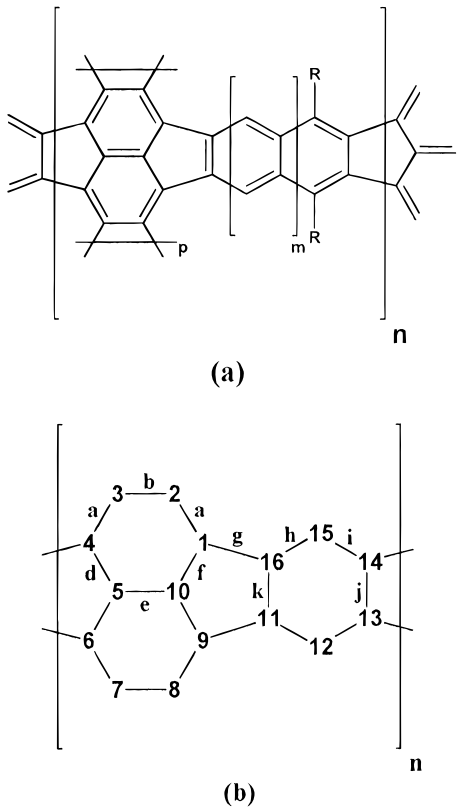

Figure 1. Unit cell of poly(fluoranthene), PFA, polymers. (a) General formula. p is the number of rings in the perpendicular oligoacenic fragments, and $m + 1$ is the number of parallel ones. Schlüter et al.[1] have made polymers with $p = 2$ and $m = 0$ and 2. (b) Labeling of the $p = 2$, $m = 0$ case.

We have performed similar LHS calculations on selected conjugated polymers and many conjugated molecules, including finite fluoranthenes. We found a very good correlation between the calculated HOMO−LUMO gap and the lowest energy absorption peaks.[11,13] A few test cases are displayed in Figure 2.

A further advantage of this approach is that it allows the approximate decomposition of the band gap into a topological, E_g^{topol}, and a relaxation, E_g^{relax}, contribution. The topological gap refers to a geometry in which all

[⊗] Abstract published in *Advance ACS Abstracts,* December 15, 1995.

0024-9297/96/2229-0940$12.00/0

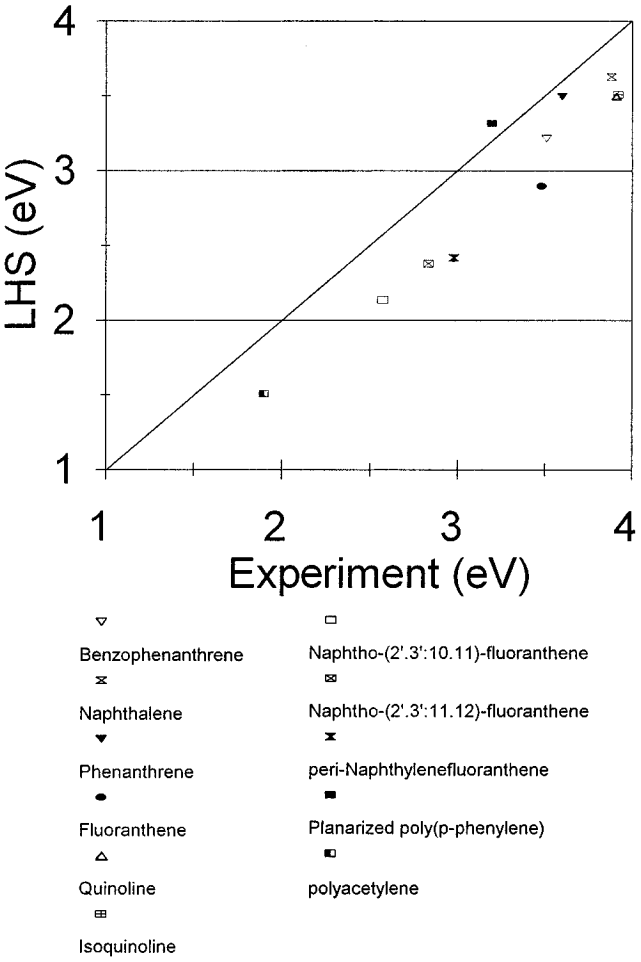

Figure 2. Comparison of LHS calculated band gaps with experimental lowest energy transitions or band gaps of selected conjugated molecules and polymers.

Table 1. Bond Distances (Å) for the Fluoranthene Molecule (FA) and Polyfluoranthene (PFA)

bond type (Figure 1b)	X-ray for FA[14]	LHS optimized geometry	
		FA	PFA
g	1.476	1.472	1.471
a	1.372	1.390	1.393
b	1.407	1.420	1.416
i	1.383	1.398	1.405
h	1.388	1.407	1.405

CC bond distances are assumed to be equal (1.40 Å), while the relaxed calculation refers to the fully optimized geometry.

The success of this approach is due to the fact that tight binding Hamiltonians, such as LHS that is being used here, can properly account for a number of important factors entering into the electronic energy levels. This can be expressed for the band gap as an approximate perturbation formula[6,7,10]

$$E_g \approx E_g^{\text{topol}} + E_g^{\text{relax}} + E_g^{\text{heteroat}} + E_g^{\text{nonplan}} + E_g^{\text{ring}} + E_g^{\text{h.n.}}$$

where each term corresponds to a separate perturbation resulting from the incorporation of the following effects (in the above order): topology, geometry relaxation, heteroatom substitution, nonplanarity (torsion), ring strain, and second or higher neighbor interactions. (The above formula is used for analysis, not for actual calculations.) In Peierls systems $E_g^{\text{topol}} = 0$ and E_g^{relax} becomes the Peierls gap.[7−9,12] In the ladder polymers studied in this paper, E_g^{relax} is usually substantial, typically amounting to about $^1/_2$ eV, which is a reflection of the strong coupling of the electrons to in-plane CC skeletal vibrations in these materials. This necessitates full geometry optimization whenever reasonable agreement with experiment is to be obtained.

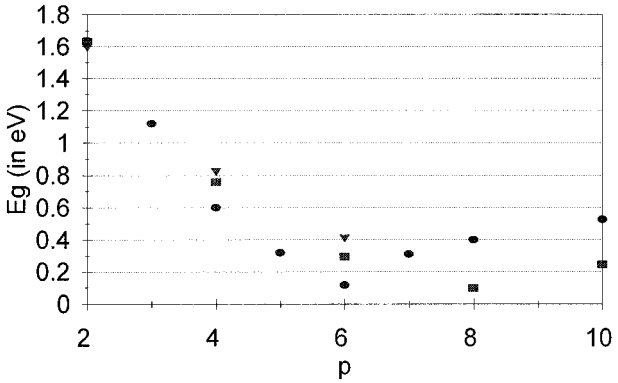

Figure 3. Energy band gap, E_g, of PFA's, as a function of p. The three different symbols refer to the $m = 0$ (circle), $m = 1$ (square), and $m = 2$ (triangle) series.

In the calculations the nonconjugated R groups have been replaced by hydrogens. Parametrization has been taken from the work of Surján et al.[11]

Periodic boundary calculations have been used throughout. We have used 11 k-points in the Brillouin zone, except in the very large unit cell calculations where 7 proved to be adequate. We have checked convergency of the bipolaronic results (section 4) and the sp^3 conjugation interruption defect calculations (section 5). The geometry and atomic charges of the carbons farthest from the defect have reached convergency up to 4 significant figures for repeat units containing 9 chemical repeat units. We report results obtained with 11 or more chemical repeat units for both bipolarons and for localized defects. The latter have been modeled by assuming that the defect turns an sp^2 carbon into an sp^3 carbon. Such defects occur naturally in the synthetic process[1] due to possibly incomplete dehydrogenation. LHS can model this type of defect by simply omitting the sp^3 carbon in question.

LHS has been used in a large number of cases to approximately calculate the CC bond distances in conjugated polymers. In Table 1 we compare some typical CC bond distances in fluoranthene and polyfluoranthene ($p = 2$, $m = 0$) and compare them with the experimental values for fluoranthene.[14] The agreement for fluoranthene itself with experiment is remarkable, considering the simplicity of the model. More significantly, the difference between fluoranthene and the polymer is quite small, aside from the obvious change of symmetry. This rather small difference between the polymer and monomer geometry is indicative of the significant degree of electron localization to the $4n + 2$ membered benzenoid and oligoacenic fragments in this polymer.

3. Band Gap Engineering

Figure 3 shows the dependence of the calculated band gap as a function of p, the length of the oligoacenic fragments of the polymer, that are perpendicular to the polymer chain. Since the geometrical relaxation is significant, the electronic structure obtained from a purely topological calculation would not be reliable. The topological band gap values follow a similar trend, as

Table 2. Variation of the Fully Relaxed Band Gap (LHS) and the Topological Band Gap as a Function of p, the Number of "Vertical" Polyacenic Rings in the Unit Cell of PFA (in eV)

	$m = 0$		$m = 1$	
p	LHS	topological	LHS	topological
2	1.637	1.062	1.633	1.066
4	0.601	0.086	0.760	0.264
6	0.118	0.285	0.293	0.051
8	0.401	0.454	0.098	0.199
10	0.527	0.478	0.245	0.277

far as band gap values are concerned, although the minimum gap occurs at a smaller value of p (see Table 2).

The three sets of symbols in Figure 3 correspond to the three series: $m = 0$ (benzene), $m = 1$ (naphthalene), and $m = 2$ (anthracene), where m, as before, denotes the size of the parallel oligoacenes that are joined to the perpendicular ones by five-membered rings. In all these cases, first there is a decreasing trend for the gap up until $p = 6$ for the $m = 0$ series and $p = 8$ for the $m = 1$ series, followed by an increasing trend for larger sized perpendicular oligoacenic groups. For the $m = 2$ series the minimum occurs for $p > 6$. The most attractive target for synthesizing a reduced band gap member of the PFA family corresponds to $m = 0$, $p = 4$ or 6.

The V-shaped dependence of E_g on p can be readily understood by inspecting the frontier orbitals of the $m = 0$ series. A level crossing occurs between $p = 4$ and 6, as shown in Figure 4. This crossover is a consequence of the topology of the system and occurs already for the nonrelaxed, "topological" calculation. We have also studied polymers with oligoacenic components corresponding to odd numbers of rings, which are nonsymmetrical with respect to the polymer chain axis. Band gaps corresponding to $p = 3$, 5, and 7 (all $m = 0$) in Figure 3 refer to such structures, but do not seem to produce significantly new trends.

The optical absorption edge for the simplest poly(fluoranthene) ($p = 2$, $m = 0$) has been measured by Schlüter et al.[1] The absorption spectrum has an ill-defined extended peak in the 550−600 nm region (∼2.2 eV). Since no information about the chain length or conjugation length distribution is known for this material, it is reasonable to conclude that the calculated band gap for the infinite PFA ($p = 2$, $m = 0$) of 1.63 eV should be lower than the experimental transition energy of the finite chains and therefore can be brought into qualitative agreement with the available experimental data only if we assume that the chain length or conjugation length are not infinitely long. This interpretation leaves some room for further reduction of the band gap by improvement of the material (longer chains, less defects) for the $p = 2$, $m = 0$ Schlüter-type polymer, although in view of the correlation between LHS and experiment shown in Figure 2, this reduction is expected to be in the range of a few tenths of an electronvolt only.

The case of the $p = 2$, $m = 2$ material is different from this point of view. The absorption peak[2] is sharper than for the $m = 0$ case and occurs also at a slightly lower energy, at ∼1.9 eV. The calculated band gap values for the $p = 2$ polymers are very similar, being almost independent of the m value. We conclude that the most likely explanation of the differences between the observed spectral band edges of the $m = 0$ and $m = 2$ polymers is more related to the conjugation defects or other limitations of the conjugation length rather than to the differences in the intrinsic bulk band gap values.

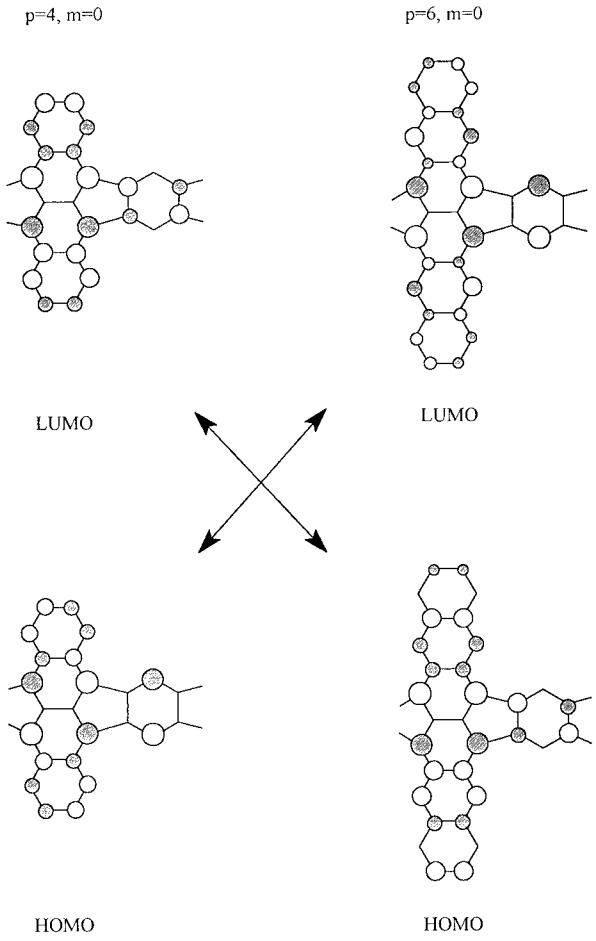

Figure 4. Frontier orbitals of the repeat units of PFA showing a level crossing from the polymer $p = 4$ to $p = 6$ ($m = 0$).

The geometry of PFA's as a function of p displays a very interesting trend, as illustrated for the $m = 0$ case in Figure 5a. (The trend for the $m = 1$ case is very similar, see Figure 5b.) For $p = 2$, $m = 0$ (one of the experimentally synthesized polymers), the connecting five-membered ring has the longest CC bond, indicating that the electrons in the two kinds of oligoacenic fragments are localized to some extent. This localization on the $4n + 2$ Huckel-type substructures, i.e. in the oligoacenic fragments, is characteristic for the $p = 2$ series. This explains not only that the longest bonds occur in the five-membered rings but also the trends of the high degree of localization of the bipolarons, as discussed in the next section, and the observation about the rather small calculated difference between the geometry of the monomer and polymer, as discussed in section 2. However, with increasing p values the longest CC bond (g) decreases, indicating a better delocalization across the five-membered rings. Around the crossover point, discussed above, π-conjugation increases and the band gap decreases. (For even larger p values the band gap will eventually approach the limiting value of polyacenes, which is estimated to be around 0.4 eV.[15] Since long polyacenes are not stable, this limit has only theoretical implications.)

Another tool available for band gap "engineering" is heteroatomic substitutions. According to our calculations on five different substituted polyfluoranthene polymers, pyridine-type nitrogen substitutions produce shifts in the +0.2 to −0.15 eV range. These substitu-

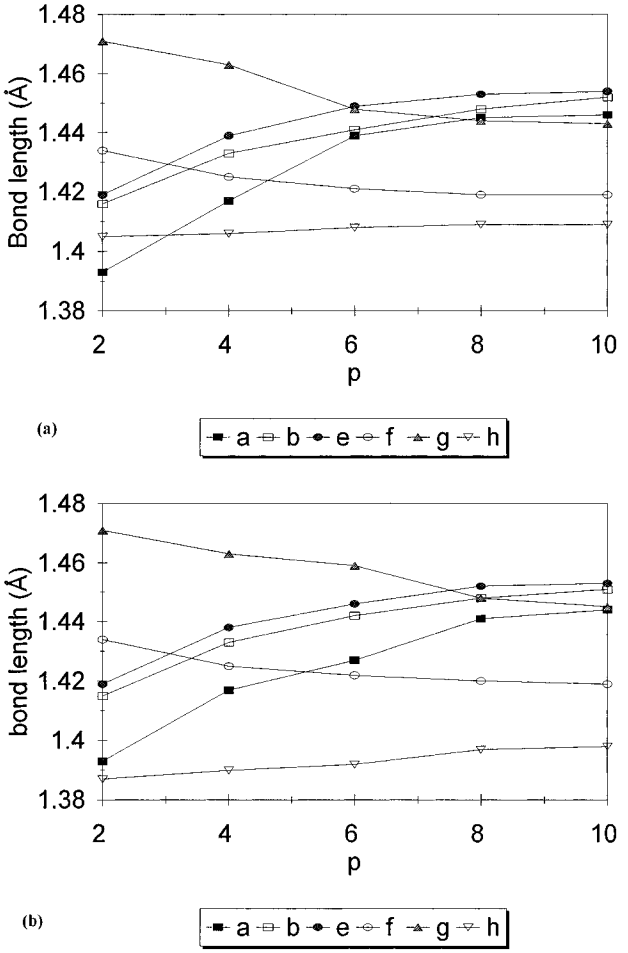

Figure 5. Variation of the CC bond distances as a function of p, the number of rings in the perpendicular oligoacenic fragments of poly(fluoroanthene) polymers: (a) $m = 0$ series; (b) $m = 1$ series. (Numbering according to Figure 1b.)

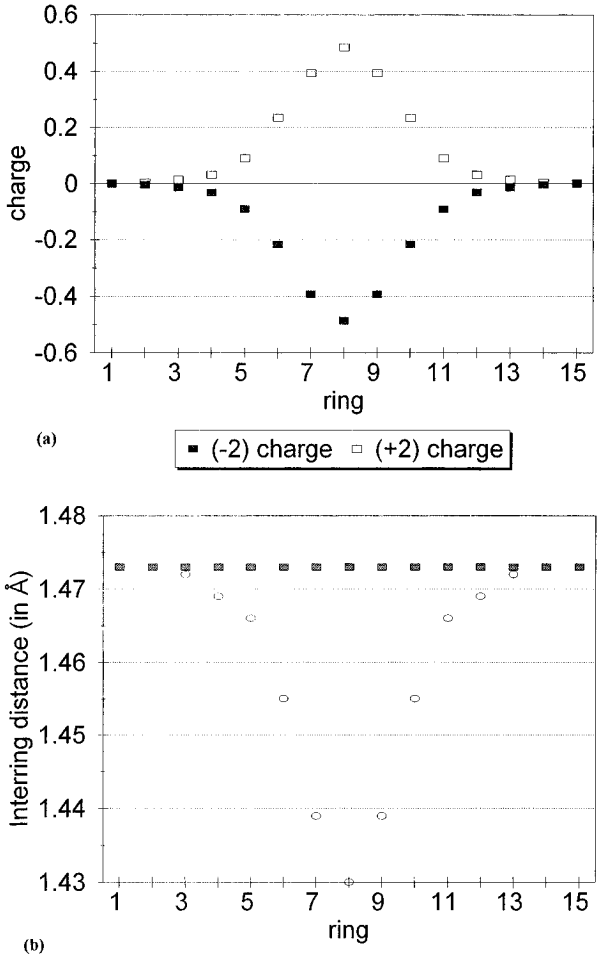

Figure 6. Bipolarons in poly(*p*-phenylene), PPP. Calculations refer to both positive and negative bipolarons. (a) Charges along the supercell of 15 rings. (b) Inter-ring bond distances (Å). The upper line indicates the value without the bipolaron.

tional effects follow the patterns of the frontier orbitals; the smallest band gap corresponds to the substitution at the C_{15} carbon site and is 1.5 eV for the $p = 2$, $m = 0$ case. Most interesting would be to explore experimentally those cases, in which the three effects, topology, geometrical relaxation, and heteroatomic substitutions, combined together yield very small band gaps.

4. Charged Defect States: Bipolarons

We have taken advantage of the LHS technique to model charged polyfluoranthenes by placing two additional electrons in the physical unit cell (supercell), consisting of up to 11 chemical repeat units, while maintaining periodic boundary conditions. (The largest calculation referred to a unit cell of 176 sp^2 carbons. As mentioned in section 2, this calculation can be considered sufficiently converged.)

For comparative purposes we have performed similar calculations on charged poly(*p*-phenylene), with 15 phenylene units constituting the supercell (both +2 and −2). The results are shown in Figure 6. These show the following trends:

(1) There is full symmetry between the positively and negatively charged bipolarons, in agreement with the fact that PPP is an alternant hydrocarbon and the LHS model in such a case displays perfect electron-hole symmetry.

(2) The results are in very good agreement with the best available ab initio calculations[16] in terms of the size of the bipolaron (depending on the definition, 5 or 7 unit cells), although the center of the bipolaron has a somewhat more uniform charge distribution, according to the ab initio calculations,[16] than in ours.

(3) Our LHS calculations on the CC bond distances also agree very well with the large double ζ type ab initio calculations. The extent of the bipolaron can be also identified from Figure 6b, that shows the inter-ring CC bond distance along the supercell of 15 phenylene rings. Again, the bipolaron extends over 5−7 rings. The shortest and longest bond length values are 1.409 and 1.435 Å, respectively. The corresponding ab initio values are 1.395 and 1.445 Å, as estimated from Figure 5 of ref 16. The ab initio calculation shows a slight asymmetry with respect to the sign of the bipolaron, while the LHS model calculation should not and does not.

The results on the Schlüter polymers clearly show the formation-localized bipolarons, as can be seen from the pattern of bond distances shown in Figure 7. The bipolarons clearly show localization, over three unit cells (six "rings" in the figure), with very minor perturbations extending over the next two neighbors, one on each side. The degree of localization of the bipolaron for PFA is very similar to that of PPP if we take into account the fact that the unit cell in the latter case is much larger.

Another way to look at the bipolaron is to plot the charge distribution along the polymer. In Figure 8 we have plotted charges for each unit or "ring" along the chain, by adding the atomic charges for each phenylene and naphthalene unit. Accordingly, the bipolaron ex-

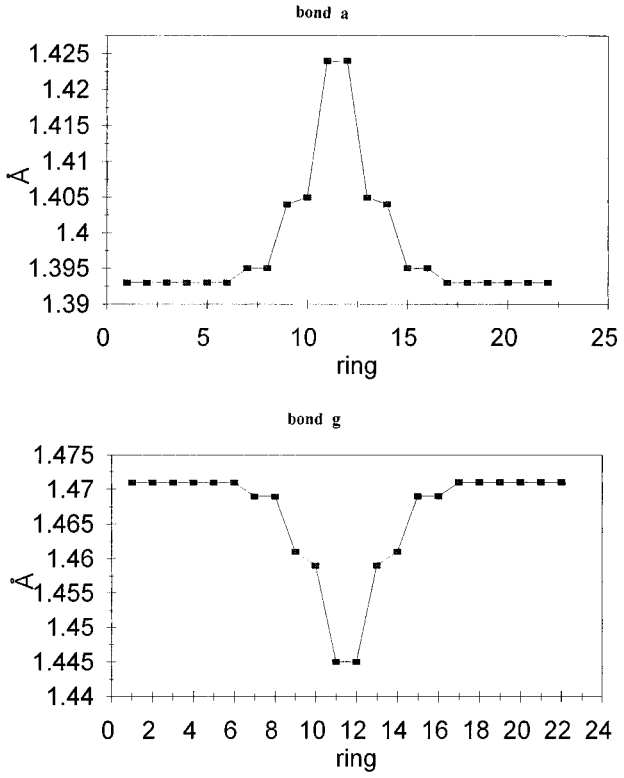

Figure 7. Variation of selected bond distances in the bipolaronic lattice calculation. The charge is −2 for the whole supercell. The bipolaron is in the middle of a supercell containing 11 chemical repeat units ($p = 2$, $m = 0$ case).

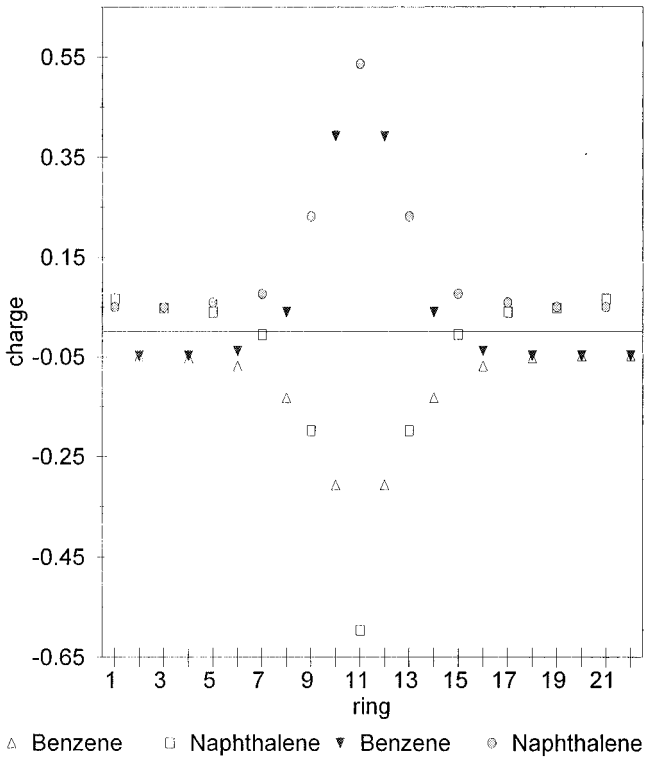

Figure 8. Variation of change distribution among naphthalenic and benzenoid units in the bipolaronic lattice calculation. The bipolaron is in the middle of a supercell containing 11 chemical repeat units ($p = 2$, $m = 0$ case). Both positive and negative bipolarons are given.

tends over 5−7 oligoacenic groups (benzene and naphthalene groups), although the charge distribution is more peaked around the center than in PPP. As one moves away from the center of the defect, the "ring" charges converge to the same value independently of the sign of the charge of the bipolaron, clearly indicating that the size of the bipolaron is about 7 "rings", i.e. $3^1/_2$ unit cells.

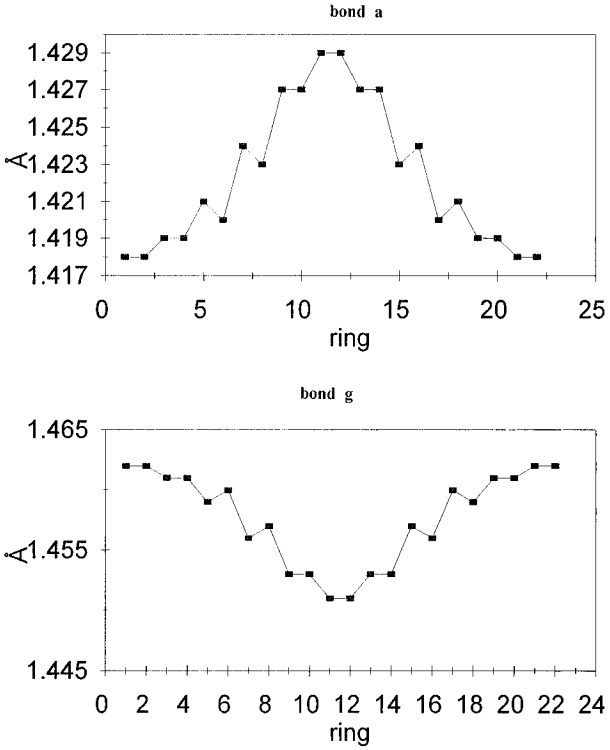

Figure 9. Variation of selected bond distances in the bipolaronic lattice calculation. The (2−) bipolaron is in the middle of a supercell containing 11 chemical repeat units ($p = 4$, $m = 0$ case). (Connecting lines are provided to guide the eye.)

The symmetry with respect to the sign of the bipolaron has been lost, of course, relative to PPP, since due to the presence of five-membered rings the PFA's are nonalternant hydrocarbons.

What is the influence of the band gap on the degree of localization of the bipolaron? It follows from very general considerations that the bipolaron should be completely delocalized for zero band gap and should be completely localized to one unit cell for a molecular species for which there is no significant coupling between the unit cells. In order to assess this question more quantitatively, we have also plotted the bipolaron bond distance distribution for two bonds for the $p = 4$, $m = 0$ polymer, which has a band gap less than half of that of the $p = 2$, $m = 0$ system. The results, plotted in Figure 9, show a defect extending over about 7−9 unit cells. This is a much more delocalized defect than in the $p = 2$, $m = 0$ case (Figure 7) by about a factor of 2. Since the amount of charge is the same, the deformations of the bonds relative to the uncharged polymer are smaller than in the larger gap polymer. This indicates that the bond distance relaxation of the small band gap polymers will be smaller in magnitude but more extended than that of their large band gap relatives.

5. Conjugation sp^3 Defects

The role of sp^3-type carbon defects may be less significant in PFA polymers than in single main chain polymers, such as poly(*p*-phenylene), given their ladder topology. Intuitively, one may assume that as long as one of the two "legs" of the ladder topology remains available for π-conjugation, the on-chain conductivity may be maintained.[17] It is relatively straightforward

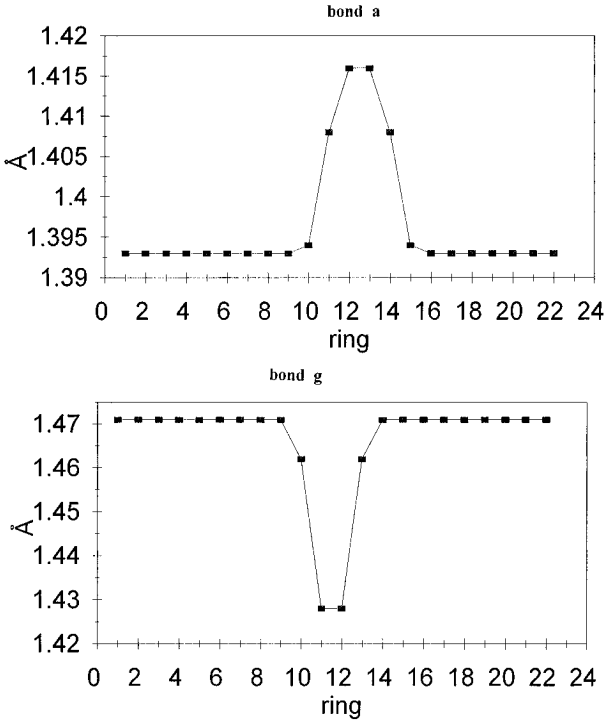

Figure 10. Variation of selected bond distances in the polaronic lattice calculation. The polaron is in the middle of a supercell containing 11 chemical repeat units ($p = 2$, $m = 0$ case). The charged (spinless) polaron arises due to an sp^3 defect at a C_{15} carbon. (Numbering refers to Figure 1b.)

to model such defects in the LHS scheme. For instance, C_{15} can be transformed into an sp^3-type carbon by eliminating π-bonds h and i in the unit cell. Such a defect will not remain localized, and it leads to a polaronic defect once the lattice is allowed to relax. We have performed a limited number of such simulations. The charge distribution and bond relaxation pattern, corresponding to such a defect for the ($m = 0$, $p = 2$) PFA polymer is shown in Figure 10. The charge distribution extends over only four rings, and is therefore somewhat more localized than in the case of a bipolaron (Figures 7 and 8).

An important issue is, how does the makeup of the repeat unit influence this localization? We have compared the charge distribution of the polaron for two cases, the $m = 0$, $p = 2$ and the $m = 0$, $p = 4$ case. The latter has a much smaller band gap, and the corresponding polaron extends over 7 or more units. This conclusion is very similar to the dependence of the size of the bipolaron on the band gap. In both cases, small band gaps tend to produce less localized defects, thus providing a mechanism for reduced scattering of sp^3 defects in ladder polymers, which should enhance their electrical conductivities.

Acknowledgment. This work has been partially supported by NSF through Grant No. DMR-9115548.

References and Notes

(1) Schlüter, A. D.; Loffler, M.; Enkelman, V. *Nature* **1994**, *368*, 831.
(2) Loffler, M.; Schlüter, A. D.; Gessler, K.; Saenger, W.; Toussaint, J.-M.; Bredas, J.-L. *Angew. Chem., Int. Ed. Engl.* **1994**, *33*, 2209.
(3) Scherf, U.; Müllen, K. *Synthesis*, **1992**, 23. Scherf, U.; Müllen, K. *Polymer* **1992**, *33*, 2443.
(4) Ladder-type polymers of buckminsterfullerene have been described by various groups: Ecklund, P. C.; et al. *Science* **1993**, *259*, 955. Pekker, S.; et al. *Ibid.* **1994**, *265*, 1077. Nunez-Regueiro, M.; Marques, L.; Hodeau, O.; Bethoux, J.-L.; Rerroux, M. *Phys. Rev. Lett.* **1995**, *74*, 278.
(5) Schlüter, A. D. *Adv. Mater.* **1991**, *3*, 282. Lamba, J. J. S.; Tour, J. M. *J. Am. Chem. Soc.* **1994**, *117*, 11723. Goldfinger, M. B.; Swager, T. M. *Ibid.* **1994**, *116*, 7895. Chmil, K.; Scherf, U. *Makromol. Chem., Rapid. Commun.* **1993**, *14*, 217.
(6) Theoretical papers on ladder polymers include: Kertesz, M.; Hoffmann, R. *Solid State Commun.* **1983**, *47*, 97. Tanaka, K.; Ohzeki, K.; Nankai, S.; Yamabe, T.; Shirakawa, H. *J. Phys. Chem. Solids* **1983**, *44*, 1069. Hong, S. Y.; Kertesz, M.; Lee, Y. S.; Kim, O.-K. *Chem. Mater.* **1992**, *4*, 378. Toussaint, J. M.; Bredas, J.-L. *Synth. Met.* **1992**, *46*, 325. Liegener, C. M.; Bakhshi, A. K.; Ladik, J. *Chem. Phys. Lett.* **1992**, *199*, 62. Bakhshi, A. K.; Liegener, C. M.; Ladik, J. *Chem. Phys.* **1993**, *173*, 65. Karabunarliev, S.; Gherghel, L.; Koch, K.-H.; Baumgarten, M. *Chem. Phys.* **1994**, *189*, 53. Kertesz, M. *Macromolecules* **1995**, *28*, 1475.
(7) Lee, Y. S.; Kertesz, M. *J. Chem. Phys.* **1988**, *88*, 2609.
(8) See, e.g.: Chance, R. R.; Boudreaux, D. S.; Brédas, J.-L.; Silbey, R. In *Handbook of Conducting Polymers*; Skotheim, T. A., Ed.; Dekker: New York, 1986; p 823.
(9) Bredas, J.-L. *Springer Ser. Solid-State Sci.* **1985**, *63*, 166. Brédas, J.-L.; Heeger, A. J.; Wudl, F. *J. Chem. Phys.* **1986**, *85*, 4673.
(10) Hong, S. Y.; Marynick, D. S. *J. Chem. Phys.* **1992**, *96*, 5497.
(11) Kertesz, M.; Surján, P. R. *Solid State Commun.* **1981**, *39*, 611. Boudreaux, D. S.; Chance, R. R.; Frommer, J. E.; Bredas, J.-L.; Silbey, R. *Phys. Rev.* **1985**, *B31*, 652. Kürti, J.; Surján, P. R. *J. Chem. Phys.* **1990**, *92*, 3247. Kürti, J.; Surján, P. R.; Kertesz, M. *J. Am. Chem. Soc.* **1991**, *113*, 9865.
(12) Longuet-Higgins, H. C.; Salem, L. *Proc. R. Soc. London* **1959**, *A251*, 172.
(13) Clar, E. *Polycyclic Hydrocarbons*; Academic Press: New York, 1964.
(14) Hazell, A. C.; Jones, D. W.; Sowden, J. M. *Acta Crystallogr.* **1977**, *B33*, 1516.
(15) Gyul'maliev, A. M. *Russ. J. Phys. Chem.* **1986**, *60*, 1008.
(16) Ehrendorfer, Ch.; Karpfen, A. *J. Phys. Chem.* **1995**, *99*, 10196.
(17) Conwell, E. M.; Mizes, H. *Phys. Rev.* **1991**, *B44*, 3963.

MA951232Z